Original Article

Histone H3 trimethylation on lysine 27 immunostaining pattern in *DICER1*-associated tumors

Murad Alturkustani[1,2,3,4#], Bo Yang[1,5#], Crystal Bockoven[1,2], Roshan Mahabir[1,2], Nick Shillingford[1,2], Ryan J. Schmidt[1,2], Shengmei Zhou[1,2], Mikako Warren[1,2], David M. Parham[*], Bruce Pawel[1,2], Larry L. Wang[1,2]

[1]Department of Pathology and Laboratory Medicine, Children's Hospital Los Angeles, Los Angeles, CA, USA; [2]Keck School of Medicine, University of Southern California, Los Angeles, CA, USA; [3]King Abdulaziz University, Jeddah, Saudi Arabia; [4]University of Western Ontario, London, ON, Canada; [5]Department of Pathology, Tianjin Medical University Cancer Institute and Hospital, National Clinical Research Center for Cancer, Key Laboratory of Cancer Prevention and Therapy, Tianjin's Clinical Research Center for Cancer, Tianjin, China

Contributions: (I) Conception and design: M Alturkustani, LL Wang; (II) Administrative support: LL Wang; (III) Provision of study materials or patients: LL Wang, M Warren, N Shillingford, B Pawel, DM Parham; (IV) Collection and assembly of data: M Alturkustani, B Yang, LL Wang; (V) Data analysis and interpretation: M Alturkustani, B Yang, LL Wang; (VI) Manuscript writing: All authors; (VII) Final approval of manuscript: All authors.

[#]These authors contributed equally to this work.

Correspondence to: Larry L. Wang, MD, PhD. Department of Pathology and Laboratory Medicine, Children's Hospital Los Angeles, Los Angeles, CA, USA; Keck School of Medicine, University of Southern California, 4650 Sunset Boulevard, MS#43, Los Angeles, CA 90027, USA.
Email: lawang@chla.usc.edu.

Background: *DICER1*-associated tumors are heterogeneous and affect several organs. *DICER1*-associated primary intracranial sarcoma is associated with histone H3 trimethylation on lysine 27 (H3K27me3) loss in nucleus by immunohistochemistry.

Methods: We explored the H3K27me3 immunostaining pattern in other *DICER1*-associated tumors. Twelve tumors from eleven patients with confirmed *DICER1* mutations (sporadic and germline) data from a pancancer next-generation sequencing panel, and four tumors of pleuropulmonary blastoma (PPB) were retrieved from our database and stained with anti-H3K27me3 antibody.

Results: The H3K27me3 expression in the nucleus showed heterogeneous mosaic loss in neoplastic Sertoli cell components in three of the five cases of moderately to poorly differentiated Sertoli-Leydig cell tumors. Among two tumors of *DICER1*-associated primary intracranial sarcoma, one showed complete loss of H3K27me3 in all neoplastic cells, whereas the other showed mosaic loss in the sarcomatous spindle cells. One *DICER1*-associated tumor with epithelial and mesenchymal differentiation, including pulmonary blastoma and PPB, showed mosaic loss of glandular epithelial and mesenchymal components. Four cases of type II PPB and a single case of type III PPB showed a similar mosaic loss of H3K27me3 staining restricted to large spindle cell components. All other components in all tumors—including Leydig cells; the areas of epithelial, cartilaginous, and rhabdomyomatous differentiation; and all cells of the remaining three cases (one papillary thyroid carcinoma and two cases of PPB type I)—demonstrated retained H3K27me3 staining.

Conclusions: H3K27me3 expression is not universally lost in *DICER1*-associated tumors and thus is not predictive of *DICER1* mutation status. The mosaic regional loss of H3K27me3 immunostaining is consistent in PPB type II and III, which can be a helpful diagnostic marker for these tumors and suggests a similarity to *DICER1*-associated intracranial sarcoma.

Keywords: *DICER1*; histone H3 trimethylation on lysine 27 (H3K27me3); immunohistochemistry; pleuropulmonary blastoma (PPB); Sertoli-Leydig cell tumor

[*] retried, used to work in Department of Pathology and Laboratory Medicine, Children's Hospital Los Angeles, Los Angeles, CA, USA.

Submitted Feb 27, 2024. Accepted for publication Apr 09, 2024. Published online Apr 28, 2024.
doi: 10.21037/tp-24-61
View this article at: https://dx.doi.org/10.21037/tp-24-61

Introduction

DICER1 is a gene that encodes the protein DICER1, that is a cytoplasmic RNase III enzyme that is essential for microRNA (miRNA) production and RNA-induced silencing complex formation, which silences messenger RNA (mRNA) expression (1). *DICER1*-associated tumors comprise a heterogenous group that affects many organs including pleuropulmonary blastoma (PPB), cystic nephroma, Wilms tumor, Sertoli-Leydig cell tumor, uterine cervical embryonal rhabdomyosarcoma, multinodular goiter, nasal chondromesenchymal hamartoma, pineoblastoma, pituitary blastoma, ciliary body medulloepithelioma, embryonal tumor with multilayered rosette (ETMR)-like infantile cerebellar tumor, *DICER1*-associated primary intracranial sarcoma, and other rare entities (1-10). Kamihara *et al.* (11) recently described five *DICER1*-associated primary intracranial sarcomas with consistent loss of histone H3 trimethylation on lysine 27 (H3K27me3) immunostaining in the nucleus. This was confirmed by Alexandrescu *et al.* (12) who reported six *DICER1*-associated primary intracranial sarcomas showed diffuse (n=4), mosaic (n=1) or minimal (≤5%, n=1) loss of H3K27me3 and nuclear TLE1 expression (n=6), which implied that the combination of H3K27me3 and TLE1 immunostaining can be helpful diagnostic markers for *DICER1*-associated primary intracranial sarcomas, and a similar loss in two additional *DICER1*-associated tumors (ETMR-like infantile cerebellar tumor and pineoblastoma) and a case of PPB type II. However, the H3K27me3 immunostaining status in other *DICER1*-associated tumors remains unknown.

The association between *DICER1* and H3K27me3 is unclear, but linkages have been described. Ting *et al.* (13) reported the importance of intact DICER for the maintenance of CpG island hypermethylation status in HCT116 human colon cancer cells with DICER helicase domain knockout, and H3K27me3 showed a small but consistent decrease across the entire promoter region at the DICER-regulated *SFRP4* and *ICAM-1* promoters, suggesting that the changes in chromatin modifications could be characteristic of the DICER-target genes. Kanellopoulou *et al.* (14) found that in the absence of Dicer (a mouse analog of DICER), there was a marked reduction in SUZ12, JARID2, and H3K27me3 at the transcriptional start sites in $DCR^{-/-}$ mouse embryonic stem cells.

In this study, we explored the H3K27me3 staining pattern in *DICER1*-associated tumors, investigated the correlation between this staining pattern and *DICER1* mutations, and assessed whether it can be used to predict *DICER1* status in these tumors. We present this article in accordance with the MDAR reporting checklist (available at https://tp.amegroups.com/article/view/10.21037/tp-24-61/rc).

Highlight box

Key findings

- The mosaic regional loss of H3 trimethylation on lysine 27 (H3K27me3) immunostaining is consistent for pleuropulmonary blastoma (PPB) type II and III.

What is known and what is new?

- According to immunohistochemistry, *DICER1*-associated primary intracranial sarcoma is correlated with H3K27me3 loss in the nucleus.
- H3K27me3 expression is not universally lost across *DICER1*-associated tumors.

What is the implication, and what should change now?

- H3K27me3 expression is not predictive of *DICER1* mutation status. The mosaic regional loss of H3K27me3 immunostaining can be a helpful diagnostic marker for PPB type II and III.

Methods

The study was conducted in accordance with the Declaration of Helsinki (as revised in 2013). Institutional review board approval from Children's Hospital Los Angeles (IRB Approval: CHLA-15-00067-CR008) was obtained for this study. Informed consent was taken from all the patients. Twelve tumors from 11 patients with confirmed *DICER1* mutations (sporadic and germline) data were retrieved from the Department of Pathology and Laboratory Medicine archives at Children's Hospital Los Angeles, including from patients with ovarian Sertoli-Leydig cell tumors (n=5), *DICER1*-associated intracranial sarcoma (n=2), *DICER1*-associated tumor with epithelial and mesenchymal differentiation (n=1), PPB (n=3), and papillary thyroid carcinoma (n=1). Four cases with a diagnosis of PPB were

included regardless of *DICER1* status because of their high association with *DICER1* alteration and their resemblance to *DICER1*-associated primary intracranial sarcoma.

Genetic mutational data were obtained from the results of a pancancer next-generation sequencing panel, OncoKids (the OncoKids panel is an amplification-based next-generation sequencing assay designed to detect diagnostic, prognostic, and therapeutic markers across the spectrum of pediatric malignancies, including leukemia, sarcomas, brain tumors, and embryonal tumors). The DNA content of this panel covered the full coding regions of 44 cancer predisposition loci, tumor-suppressor genes, and oncogenes; hotspots for mutations in 82 genes; and amplification events in 24 genes. The RNA content includes 1,421 targeted gene fusions (15) and chromosomal microarray analysis (CMA) (16).

Representative sections from each tumor were stained with an anti-H3K27me3 antibody (Cat. #9733S; antibody clone number: C36B11; dilution: 1:75; Cell Signaling Technology, Danvers, MA, USA). Slide preparation was performed in our Clinical Laboratory Improvement Amendments (CLIA)-certified laboratory in accordance with a standardized operating procedure. The malignant peripheral nerve sheath tumor (MPNST) with completely lost in all neoplastic cells was used as negative control. Patients with no available blocks were excluded from this study. The related clinicopathological and molecular features were reviewed.

The staining patterns for H3K27me3 were defined as follows: (I) staining in less than 5% of the cells of interest was considered complete loss of staining; (II) 5–95% staining in the cells of interest was considered heterogeneous mosaic loss of staining; and (III) more than 95% staining in the cells of interest was considered complete retention of staining.

Results

Sixteen tumors from 15 patients met the inclusion criteria (*Table 1*). These included five cases of ovarian Sertoli-Leydig cell tumors, two cases of *DICER1*-associated intracranial sarcoma, one case of *DICER1*-associated tumor with epithelial and mesenchymal differentiation, seven cases of PPB, and one case of papillary thyroid carcinoma. The details of cases 3 (17) and 6 (16) have been described previously.

Three of the five ovarian Sertoli-Leydig cell tumors demonstrated multifocal areas of mosaic loss of H3K27me3 expression. The first two cases showed preserved nuclear staining in all neoplastic cells, including moderately-to-poorly differentiated Sertoli cells, pleomorphic cells, and heterologous epithelial components (*Figure 1A-1C*). Case 3 exhibited focal areas of cystic spaces with papillary projections, consistent with a retiform component. The stroma of these papillae showed mosaic loss of H3K27me3 staining, while all other components demonstrated preserved nuclear staining. Case 4 contained a heterologous component in the form of focal rhabdomyosarcomatous differentiation with an intact H3K27me3 staining pattern, and the loss of H3K27me3 nuclear staining was restricted to small foci of undifferentiated oval to spindled nuclei (*Figure 1D,1E*). Case 5 had heterologous epithelial and spindle cell components. The epithelial component and most of the other components of the tumor demonstrated preserved nuclear staining, and the loss of nuclear staining was restricted to the spindle cell component, particularly in the subepithelial areas (*Figure 1F-1H*). The papillary thyroid carcinoma from patient 3 showed H3K27me3 immunostaining in more than 95% of the neoplastic nuclei.

In all cases, neoplastic cells with the loss of H3K27me3 expression demonstrated a dot-like staining pattern that represented the expected methylation of one X chromosome via lyonization. This finding served as an excellent internal control for H3K27me3 staining.

Among the two cases of intracranial sarcoma, the first case showed mosaic loss of H3K27me3 in the sarcomatous spindle cells (*Figure 2A-2D*), while the second showed a complete loss in all neoplastic cells (*Figure 2E-2G*). Neoplastic growth in the first case was formed by spindled neoplastic cells with alternating hypocellular and hypercellular areas. H3K27me3 staining revealed mosaic loss in the neoplastic cells. The second brain tumor (case 7) was from a 19-year-old male patient with a known germline *TP53* mutation, but no germline *DICER1* alteration. He had anal rhabdomyosarcoma at 3 years of age. The intracranial neoplasm contained abundant spindle cells and pleomorphic anaplastic cells. H3K27me3 staining showed a complete loss of all neoplastic cells. This case exhibited copy loss on chromosome 17, which included the *SUZ12* gene that possibly contributed to the total loss of H3K27me3 expression in all neoplastic cells.

The lung mass in case 8 was from a 20-year-old female patient with history of orbital embryonal rhabdomyosarcoma at the age of 5 years. The lung tumor was biphasic and comprised both epithelial and mesenchymal components (*Figure 3A,3B*). The epithelial components included glandular and acinar structures with squamoid morulae.

Table 1 Clinicopathological and molecular features of all *DICER1*-associated tumors

No.	Age	Sex	Diagnosis	Other tumors	*DICER* alterations	Germline	H3K27me3 staining
1	14Y	F	Ovarian SLCT, moderately-to-poorly differentiated with heterologous elements	Benign thyroid nodule and hepatic nodular regenerative hyperplasia	c.3300dupA; c.5438A>G	c.3300dupA	Retained in all cells
2	4Y	F	Ovarian SLCT, moderately-to-poorly differentiated	No	c.2436+1G>A; c.5439G>T	c.2436+1G>A	Retained in all cells
3A	13Y	F	Ovarian SLCT, moderately-to-poorly differentiated	Cervical and vaginal embryonal rhabdomyosarcoma and cystic lung lesions	c.5439G>T; c.5504_5507delATCC	c.5504_5507delATCC	Mosaic loss in Sertoli cells, retained in other cells
3B	13Y	F	Papillary thyroid carcinoma	Multinodular goiter	c.5113G>A; c.5504_5507delATCC	c.5504_5507delATCC	Retained in all cells
4	14Y	F	Ovarian SLCT, moderately-to-poorly differentiated with heterologous elements	No	c.5438A>C; c.3052G>T	Negative	Mosaic loss in Sertoli cells, retained in other cells
5	16Y	F	Ovarian SLCT, moderately-to-poorly differentiated with heterologous elements	No	c.3636delA; c.5438A>C	Negative	Mosaic loss in spindle cells resembling primitive gonadal stroma, retained in other cells
6	4Y	M	*DICER1*-associated intracranial sarcoma	No	c.5439G>C; deletion in distal long arm of chromosome 14 (containing *DICER*)	Negative	Mosaic loss in large spindle cells, retained in other cells
7	19Y	M	*DICER1*-associated intracranial sarcoma with germline TP53 mutation	Anal rhabdomyosarcoma at 3 years of age	c.5425G>A; deletion in distal long arm of chromosome 14 (containing *DICER*)	Negative	Completely lost in all neoplastic cells
8	20Y	F	*DICER1*-associated tumor with epithelial and mesenchymal differentiation including pulmonary blastoma and PPB	Orbital embryonal rhabdomyosarcoma at 5 years of age	c.5425G>T; deletion in distal long arm of chromosome 14 (containing *DICER*)	Negative	Mosaic loss in glandular epithelial and mesenchymal components, retained in squamoid morulae
9	2W	M	PPB, type I	No	c.3567T>A; c.5437G>A	c.3567T>A	Retained in all cells
10	2Y	M	PPB, type I	No	Not tested	Not tested	Retained in all cells
11	3Y	M	PPB, type II	No	c.3615C>A; c.5437G>C	c.3615C>A	Mosaic loss in large spindle cells, retained in other components
12	4Y	F	PPB, type II	No	c.901C>T; c.5438A>G	c.901C>T	Mosaic loss in large spindle cells, retained in other components
13	4Y	M	PPB, type II	No	Not tested	Not tested	Mosaic loss in large spindle cells, retained in other components
14	3Y	M	PPB, type II	No	Not tested	Not tested	Mosaic loss in large spindle cells, retained in other components
15	2Y	F	PPB, type III	No	Not tested	Not tested	Mosaic loss in large spindle cells, retained in other components

H3k27me3, histone H3 trimethylation on lysine 27; Y, years; F, female; SLCT, Sertoli-Leydig cell tumor; M, male; PPB, pleuropulmonary blastoma; W, weeks.

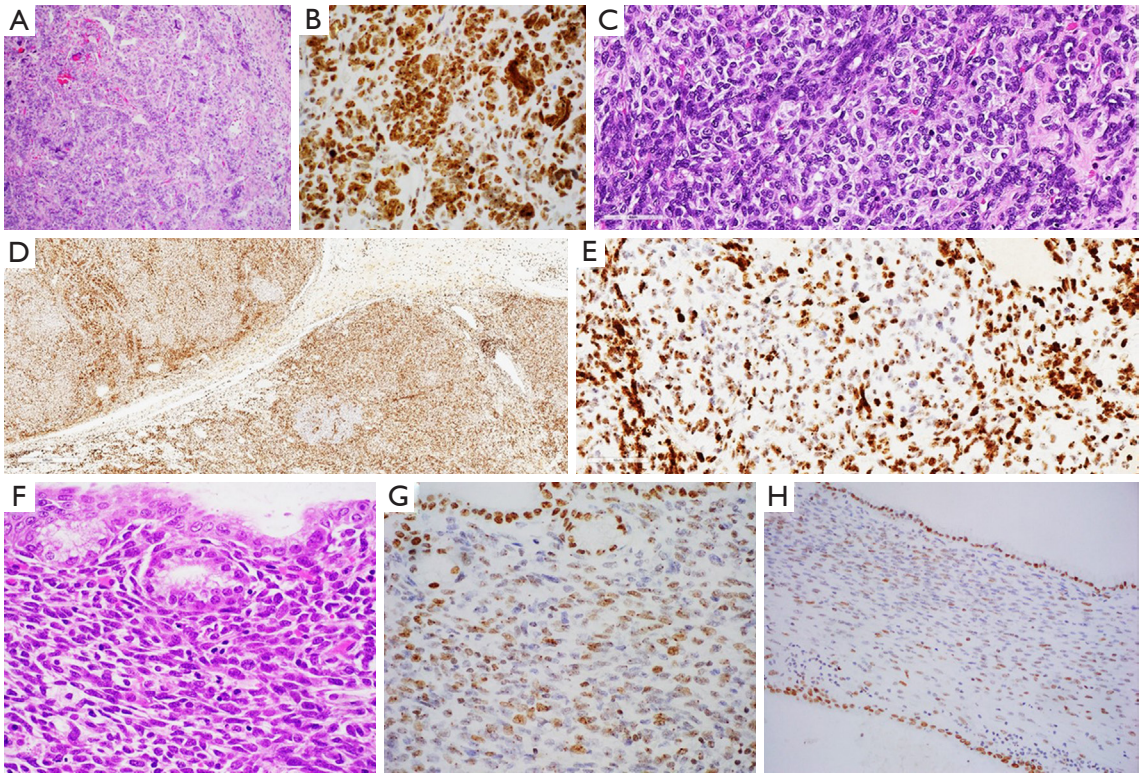

Figure 1 H3k27me3 staining pattern in ovarian Sertoli-Leydig cell tumors. (A,B) Case 1 with retained nucleus staining in most cells. (A: H&E, ×100; B: IHC, ×200). (C-E) Case 4 with mosaic loss of nucleus staining in Sertoli cells. (C: H&E, ×200; D: IHC, ×100; E: IHC, ×200). (F-H) Case 5 with mosaic loss of nucleus staining in spindle cells resembling primitive gonadal stroma. (F: H&E, ×200; G: IHC, ×200; H: IHC, ×100). H3k27me3, histone H3 trimethylation on lysine 27; H&E, hematoxylin and eosin; IHC, immunohistochemistry.

The mesenchymal component consisted of primitive round and spindle neoplastic cells. The diagnosis was *DICER1*-associated biphasic tumor with epithelial and mesenchymal differentiation, including pulmonary blastoma and PPB. As the neoplastic glandular epithelium and squamoid morulae formed part of the tumor, the diagnosis of pulmonary blastoma was favored. H3K27me3 was retained in the squamoid morulae but showed mosaic loss in other nonepithelial components with preservation of dot-like X-chromosome staining (*Figure 3C,3D*).

There were seven cases of PPB. Among the two cases of type I PPB, one had a *DICER1* mutation, whereas the other was negative for the germline *DICER1* mutation. Both showed preservation of H3K27me3 in all neoplastic cells, including septal mesenchymal cells (*Figure 4A-4D*). All four cases of type II PPB (two with *DICER1* mutations and two with an unknown *DICER1* status) and a single case of type III PPB (unknown *DICER1* status) showed similar mosaic loss of H3K27me3 staining, which was more prominent in the undifferentiated spindle cell component (*Figure 4E-4K*).

Discussion

In this study, we confirmed the previous observation of variable but consistent loss of H3K27me3 in *DICER1*-associated intracranial sarcoma, and we extended this finding to PPB type II–III. Other *DICER1*-associated tumors showed inconsistent focal mosaic nucleus staining (such as the three of five ovarian Sertoli-Leydig cell tumors) or complete retention of nuclear staining (one PPB type I and one papillary thyroid carcinoma). This result suggests that not all *DICER1*-associated tumors are associated with H3K27me3 immunostaining loss.

DICER is a cytoplasmic RNase III enzyme that is essential for miRNA and small interfering RNA (siRNA) production. DICER and miRNAs ligate and become incorporated into the RISC complex, thereby preventing mRNA expression (1). *DICER1*-associated tumors affect

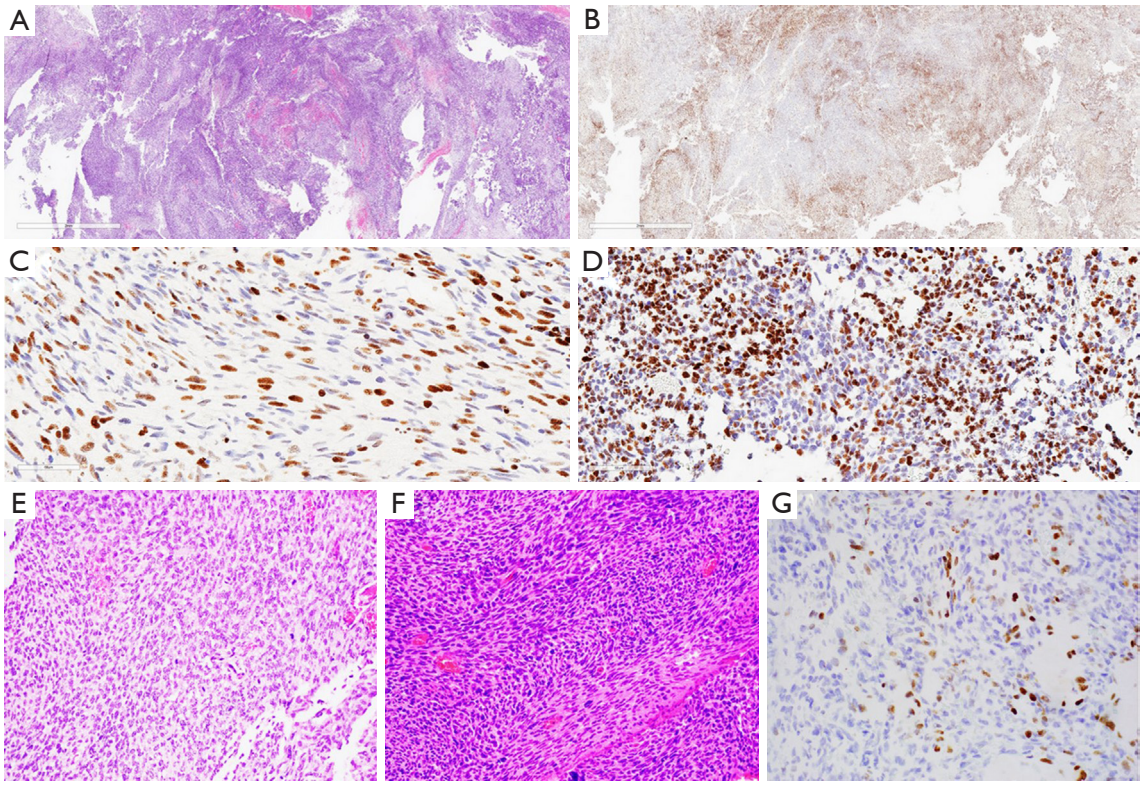

Figure 2 H3k27me3 staining pattern in *DICER1*-associated intracranial sarcoma. (A-D) Case 6: intracranial sarcoma with mosaic loss in large spindle cells. (A: H&E, ×40; B: IHC, ×40; C: IHC, ×200; D: IHC, ×100). (E-G) Case 7: intracranial sarcoma with complete loss, and only normal cells (endothelial cells, leukocytes) showed nucleus staining retention. (E: H&E, ×100; F: H&E, ×100; G: IHC, ×200). H3k27me3, histone H3 trimethylation on lysine 27; H&E, hematoxylin and eosin; IHC, immunohistochemistry.

many organs. Schultz *et al.* (2) recently described *DICER1*-associated primary intracranial sarcomas with a consistent but variable degree of loss of H3K27me3 immunostaining. This finding was confirmed by Alexandrescu *et al.* (12), who also reported a similar loss in two additional *DICER1*-associated brain tumors (ETMR-like *DICER1*-related tumor and *DICER1*-altered pineoblastoma) and a case of PPB type II. However, the H3K27me3 status in other *DICER1*-associated tumors has not yet been investigated.

Although Kamihara *et al.* (11) and Alexandrescu *et al.* (12) suggested an association between *DICER1* alteration and H3K27me3, a review of the literature failed to yield a clear and obvious correlation. A possible association was suggested by the finding that functioning DICER is required for the maintenance of CpG island hypermethylation status in human cancer cell lines (13). In mouse embryonic stem cells, the production of miR-290 miRNAs, through the functioning of DICER, plays a role in H3K27me3 methylation of *HOX* gene promoters, which is mediated through miR-290/miR-291 suppression of methyltransferase Ash1l, an antagonist of polycomb repressive complex 2 (PRC2) (14).

Trimethylation of lysine at position 27 is considered a negative regulator of gene expression. H3K27me3 expression reflects the methylation status at lysine 27 in histone 3 (18). The pattern of immunostaining for H3K27me3 can be classified as retained, mosaic/partial/heterogeneous, or completely lost. The most reliable pattern is complete loss of H3K27me3 expression in neoplastic cells, as observed in *H3F3A* K27M-mutant pediatric glioblastomas (19), group-A childhood posterior fossa ependymoma (20), and some MPNSTs (21). The underlying mechanisms in the first two tumors are similar, as aberrant expression of H3K27Mme3 and EZHIP (CXorf67) prevents PRC2 via allosteric inhibition (22). In MPNST, aberrant H3K27M and EZHIP inactivate PRC2 complex by altering its components *EED* and *SUZ12* (21).

Mosaic expression of H3K27me3 is less specific than is

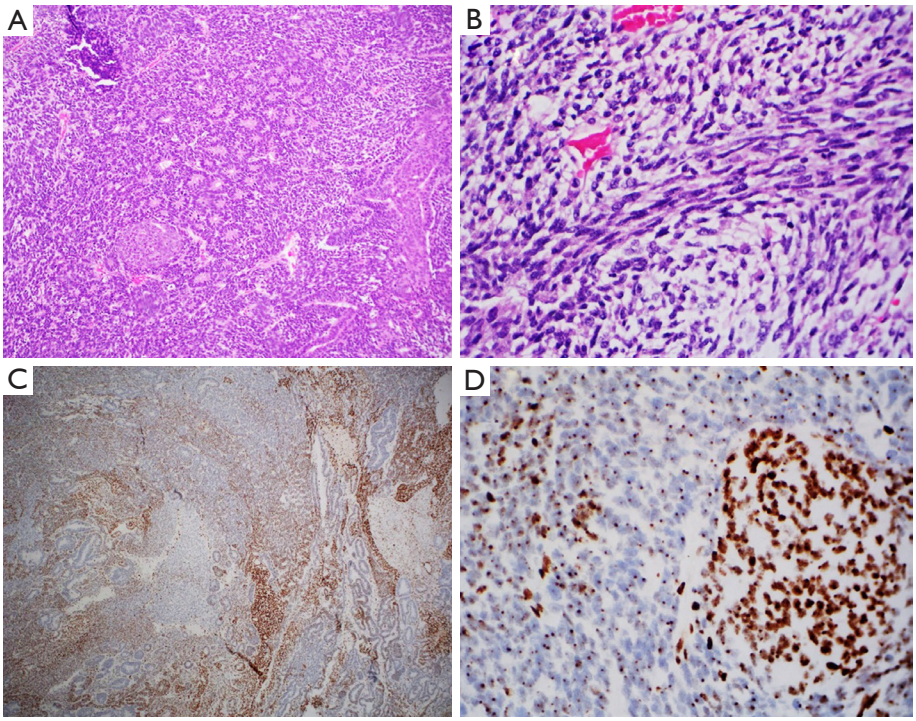

Figure 3 Case 8: *DICER1*-associated tumor with epithelial and mesenchymal differentiation. (A) Epithelial differentiation with glandular and squamoid morulae differentiation (H&E, ×100). (B) Spindle cell differentiation (H&E, ×200). (C) Mosaic loss of H3K27me3 immunostaining in glandular epithelial component (IHC, ×40). (D) Higher magnification was used to show the geographic retention of nucleus H3K27me3 immunostaining in squamoid morulae and loss except for X-chromosome dot-like staining in mesenchymal cells (IHC, ×400). H&E, hematoxylin and eosin; H3k27me3, histone H3 trimethylation on lysine 27; IHC, immunohistochemistry.

complete loss and can be observed in many different tumors such as myxofibrosarcoma, osteosarcoma, dedifferentiated liposarcoma, rhabdomyosarcoma, low-grade fibromyxoid sarcoma, leiomyosarcoma, the fibrosarcomatous variant of dermatofibrosarcoma protuberans, melanoma, neurofibroma, schwannoma, perineuroma, and ossifying fibromyxoid tumor (23). However, two patterns of mosaic expression have been described. The most common pattern is the intermingling of neoplastic cells with retained and lost staining. Geographic loss is less commonly observed and manifests as well-defined areas of loss of staining in the background of regions of retained staining. The latter pattern has been observed only in three MPNSTs and one undifferentiated pleomorphic sarcoma and is considered to be a variant of complete loss (16). The mosaic loss in the *DICER1*-associated tumors is mixed, with both intermingled loss and focal geographic loss in a subset of neoplastic cells.

Although mosaic expression of H3K27me3 can be observed in many different tumors, but they all appear in low proportions (23). The mosaic regional loss of H3K27me3 immunostaining is consistent in PPB type II and III, which can be a helpful diagnostic marker for these tumors and suggests a similarity to *DICER1*-associated intracranial sarcoma. If we suspect PPB type II and III from the tumor location and morphology, we will add H3K27me3 immunohistochemistry. If it is mosaic expression, it can be suggested that it is this tumor, so we can further do *DICER1* mutation detection to further clarify the diagnosis.

Another limitation in the interpretation of the staining results is the staining intensity. H3K27me3 deposition is a dynamic process related to the cellular stage of development, and the immunostaining process can be affected by many variables that result in different staining intensities and by a lack of agreement in the interpretation of staining patterns. These findings may explain the contradictory conclusions regarding H3K27me3 nucleus staining in synovial sarcoma. Cleven *et al.* (24) reported that 9 of 15 cases of synovial sarcoma showed loss of nuclear staining, whereas Prieto-Granada *et al.* (21) reported that none of the 113 examined cases showed loss of H3K27me3 expression.

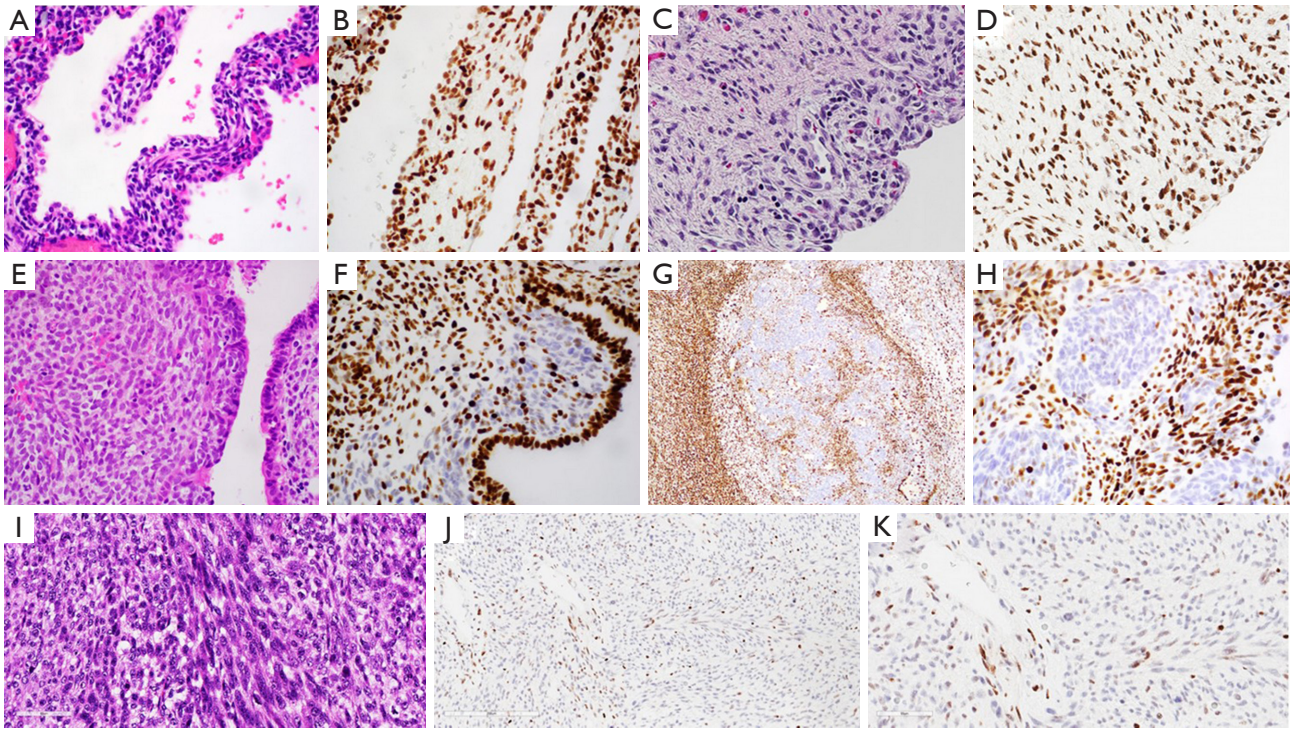

Figure 4 H3k27me3 staining pattern in PPB. (A,B) Type I (case 9), retained nucleus staining. (A: H&E, ×200; B: IHC, ×200). (C,D) Type I (case 10), retained nucleus staining. (C: H&E, ×200; D: IHC, ×200). (E-H) Type II (case 11), multifocal mosaic loss. (E: H&E, ×200; F: IHC, ×200; G: IHC, ×100; H: IHC, ×200). (I-K) Type III (case 15), more prominent mosaic loss. (I: H&E, ×200; J: IHC, ×100; K: IHC, ×200). H3k27me3, histone H3 trimethylation on lysine 27; PPB, pleuropulmonary blastoma; H&E, hematoxylin and eosin; IHC, immunohistochemistry.

In addition, Kitahama *et al.* (25) also demonstrated that using different dilutions of the same H3K27me3 antibody (clone C36B11) can result in different staining intensities and interpretations. They found that when under a 1:200 dilution, only two of 151 cases of diffuse glioma showed some degree of H3K27me3 loss, whereas under a 1:2,000 dilution, 19 of 151 cases showed H3K27me3 loss.

To reduce the potential for variable results, we restricted our interpretation to areas with well-recognized internal positive controls, such as endothelial cells and/or inflammatory cells, so that focal regions with no internal positive control were excluded in our assessment. In female patients, dot-like staining representing the methylation pattern of the X chromosome (11) was also used as an effective internal positive control.

Common features shared among cases with mosaic H3K27me3 nuclear staining in our and others' studies (11,12,19,20,23) included the following: (I) heterogenous tumors with more than one line of differentiation; (II) focal loss of the staining in areas with the least differentiation; and (III) preservation of the X-chromosome pattern of staining in female patients. The nuclei in these areas showed very faint staining compared to the X chromosome, which we considered negative. However, as we discussed regarding the threshold limitation in the interpretation of this immunostaining, the possible use of different dilutions, platforms, incubation periods, amplification methods, or other variability in the immunostaining method, may result in more intense nuclear staining and may be considered positive by other interpreters. Only one of the tumors in our series, an intracranial sarcoma, showed complete loss of nuclear immunostaining. Genetic profiling revealed evidence of loss of chromosome 17, which includes the *SUZ12* gene (a component of the PRC2 complex), which may explain the profound and total loss of H3K27me3 expression in all neoplastic cells.

Conclusions

We conclude that there is no direct/clear association between *DICER1* alteration and H3K27me3 expression, as most neoplastic cells in different *DICER1*-associated tumors retain H3K27me3 nuclear staining. Therefore, *DICER1* mutation status cannot be predicted by the immunostaining pattern of H3K27me3 alone. A possible association between *DICER1* alteration and H3K27me3 loss in these foci cannot be excluded. However, we believe that loss of H3K27me3 represents an altered epigenetic status of neoplastic cells rather than an effect of *DICER1* alteration (i.e., these findings will be present in tumors with loss of H3K27me3 regardless of *DICER1* status). We also confirmed consistent variable loss in a subset of cells in *DICER1*-associated intracranial sarcoma as a possible ancillary diagnostic aid. Mosaic regional loss of H3K27me3 immunostaining is consistent across PPB type II and III, which might be a helpful marker in the diagnostic workup of these tumors. However, the heterogeneity of the staining and the small number of cases in each category in our study preclude any meaningful conclusions. Therefore, further investigation using a larger cohort is needed to understand the significance of H3K27me3 staining.

Acknowledgments

Funding: None.

Footnote

Reporting Checklist: The authors have completed the MDAR reporting checklist. Available at https://tp.amegroups.com/article/view/10.21037/tp-24-61/rc

Data Sharing Statement: Available at https://tp.amegroups.com/article/view/10.21037/tp-24-61/dss

Peer Review File: Available at https://tp.amegroups.com/article/view/10.21037/tp-24-61/prf

Conflicts of Interest: All authors have completed the ICMJE uniform disclosure form (available at https://tp.amegroups.com/article/view/10.21037/tp-24-61/coif). The authors have no conflicts of interest to declare.

Ethical Statement: The authors are accountable for all aspects of the work in ensuring that questions related to the accuracy or integrity of any part of the work are appropriately investigated and resolved. The study was conducted in accordance with the Declaration of Helsinki (as revised in 2013). Institutional review board approval from Children's Hospital Los Angeles (IRB Approval: CHLA-15-00067-CR008) was obtained for this study. Informed consent was taken from all the patients.

References

1. Foulkes WD, Priest JR, Duchaine TF. DICER1: mutations, microRNAs and mechanisms. Nat Rev Cancer 2014;14:662-72.
2. Schultz KAP, Williams GM, Kamihara J, et al. DICER1 and Associated Conditions: Identification of At-risk Individuals and Recommended Surveillance Strategies. Clin Cancer Res 2018;24:2251-61.
3. Han LM, Weiel JJ, Longacre TA, et al. DICER1-associated Tumors in the Female Genital Tract: Molecular Basis, Clinicopathologic Features, and Differential Diagnosis. Adv Anat Pathol 2022;29:297-308.
4. Yang B, Chour W, Salazar CG, et al. Pediatric Sertoli-Leydig Cell Tumors of the Ovary: An Integrated Study of Clinicopathological Features, Pan-cancer-Targeted Next-generation Sequencing and Chromosomal Microarray Analysis From a Single Institution. Am J Surg Pathol 2024;48:194-203.
5. de Kock L, Priest JR, Foulkes WD, et al. An update on the central nervous system manifestations of DICER1 syndrome. Acta Neuropathol 2020;139:689-701.
6. de Kock L, Sabbaghian N, Druker H, et al. Germ-line and somatic DICER1 mutations in pineoblastoma. Acta Neuropathol 2014;128:583-95.
7. de Kock L, Sabbaghian N, Plourde F, et al. Pituitary blastoma: a pathognomonic feature of germ-line DICER1 mutations. Acta Neuropathol 2014;128:111-22.
8. Uro-Coste E, Masliah-Planchon J, Siegfried A, et al. ETMR-like infantile cerebellar embryonal tumors in

the extended morphologic spectrum of DICER1-related tumors. Acta Neuropathol 2019;137:175-7.
9. Koelsche C, Mynarek M, Schrimpf D, et al. Primary intracranial spindle cell sarcoma with rhabdomyosarcoma-like features share a highly distinct methylation profile and DICER1 mutations. Acta Neuropathol 2018;136:327-37.
10. Lee JC, Villanueva-Meyer JE, Ferris SP, et al. Primary intracranial sarcomas with DICER1 mutation often contain prominent eosinophilic cytoplasmic globules and can occur in the setting of neurofibromatosis type 1. Acta Neuropathol 2019;137:521-5.
11. Kamihara J, Paulson V, Breen MA, et al. DICER1-associated central nervous system sarcoma in children: comprehensive clinicopathologic and genetic analysis of a newly described rare tumor. Mod Pathol 2020;33:1910-21.
12. Alexandrescu S, Meredith DM, Lidov HG, et al. Loss of histone H3 trimethylation on lysine 27 and nuclear expression of transducin-like enhancer 1 in primary intracranial sarcoma, DICER1-mutant. Histopathology 2021;78:265-75.
13. Ting AH, Suzuki H, Cope L, et al. A requirement for DICER to maintain full promoter CpG island hypermethylation in human cancer cells. Cancer Res 2008;68:2570-5.
14. Kanellopoulou C, Gilpatrick T, Kilaru G, et al. Reprogramming of Polycomb-Mediated Gene Silencing in Embryonic Stem Cells by the miR-290 Family and the Methyltransferase Ash1l. Stem Cell Reports 2015;5:971-8.
15. Hiemenz MC, Ostrow DG, Busse TM, et al. OncoKids: A Comprehensive Next-Generation Sequencing Panel for Pediatric Malignancies. J Mol Diagn 2018;20:765-76.
16. Warren M, Hiemenz MC, Schmidt R, et al. Expanding the spectrum of dicer1-associated sarcomas. Mod Pathol 2020;33:164-74.
17. Moke DJ, Thomas SM, Hiemenz MC, et al. Three synchronous malignancies in a patient with DICER1 syndrome. Eur J Cancer 2018;93:140-3.
18. Schaefer IM, Fletcher CD, Hornick JL. Loss of H3K27 trimethylation distinguishes malignant peripheral nerve sheath tumors from histologic mimics. Mod Pathol 2016;29:4-13.
19. Venneti S, Santi M, Felicella MM, et al. A sensitive and specific histopathologic prognostic marker for H3F3A K27M mutant pediatric glioblastomas. Acta Neuropathol 2014;128:743-53.
20. Panwalkar P, Clark J, Ramaswamy V, et al. Immunohistochemical analysis of H3K27me3 demonstrates global reduction in group-A childhood posterior fossa ependymoma and is a powerful predictor of outcome. Acta Neuropathol 2017;134:705-14.
21. Prieto-Granada CN, Wiesner T, Messina JL, et al. Loss of H3K27me3 Expression Is a Highly Sensitive Marker for Sporadic and Radiation-induced MPNST. Am J Surg Pathol 2016;40:479-89.
22. Jain SU, Rashoff AQ, Krabbenhoft SD, et al. H3 K27M and EZHIP Impede H3K27-Methylation Spreading by Inhibiting Allosterically Stimulated PRC2. Mol Cell 2020;80:726-735.e7.
23. Asano N, Yoshida A, Ichikawa H, et al. Immunohistochemistry for trimethylated H3K27 in the diagnosis of malignant peripheral nerve sheath tumours. Histopathology 2017;70:385-93.
24. Cleven AH, Sannaa GA, Briaire-de Bruijn I, et al. Loss of H3K27 tri-methylation is a diagnostic marker for malignant peripheral nerve sheath tumors and an indicator for an inferior survival. Mod Pathol 2016;29:582-90.
25. Kitahama K, Iijima S, Sumiishi A, et al. Reduced H3K27me3 levels in diffuse gliomas: association with 1p/19q codeletion and difference from H3K27me3 loss in malignant peripheral nerve sheath tumors. Brain Tumor Pathol 2021;38:23-9.

(English Language Editor: J. Gray)

Cite this article as: Alturkustani M, Yang B, Bockoven C, Mahabir R, Shillingford N, Schmidt RJ, Zhou S, Warren M, Parham DM, Pawel B, Wang LL. Histone H3 trimethylation on lysine 27 immunostaining pattern in *DICER1*-associated tumors. Transl Pediatr 2024;13(4):624-633. doi: 10.21037/tp-24-61